Published in final edited form as:
Science. 2013 March 8; 339(6124): 1219–1224. doi:10.1126/science.1233913.

Aire-dependent thymic development of tumor-associated regulatory T cells*

Sven Malchow[1], **Daniel S. Leventhal**[1], **Saki Nishi**[1], **Benjamin I. Fischer**[1], **Lynn Shen**[1], **Gladell P. Paner**[1], **Ayelet S. Amit**[1], **Chulho Kang**[2], **Jenna E. Geddes**[3,#], **James P. Allison**[3,*], **Nicholas D. Socci**[4], and **Peter A. Savage**[1]

[1]Department of Pathology, University of Chicago, Chicago, IL 60637

[2]Cancer Research Laboratory, University of California, Berkeley, CA 94720

[3]Department of Immunology, Howard Hughes Medical Institute, Memorial Sloan-Kettering Cancer Center, New York, NY 10021

[4]Bioinformatics Core, Memorial Sloan-Kettering Cancer Center, New York, NY 10021

Abstract

Despite considerable interest in the modulation of tumor-associated Foxp3$^+$ regulatory T cells (Tregs) for therapeutic benefit, little is known about the developmental origins of these cells and the nature of the antigens that they recognize. Here, we identified an endogenous population of antigen-specific Tregs (termed "MJ23" Tregs) found recurrently enriched in the tumors of mice with oncogene-driven prostate cancer. MJ23 Tregs were not reactive to a tumor-specific antigen, but instead recognized a prostate-associated antigen that was present in tumor-free mice. MJ23 Tregs underwent Aire-dependent thymic development in both male and female mice. Thus Aire-mediated expression of peripheral tissue antigens drives the thymic development of a subset of organ-specific Tregs, which are likely co-opted by tumors developing within the associated organ.

Treg cells are critical for the prevention of autoimmunity, the maintenance of immune homeostasis, and the suppression of anti-tumor immune responses (1, 2). For many human cancers, the density of Tregs within tumor lesions is predictive of poor clinical outcome (3), suggesting that Tregs play a functional role in cancer progression. In this study, we set out to establish a tractable animal model in which a single specificity of naturally occurring tumor-associated Tregs could be studied in the context of a genetically driven mouse model of autochthonous cancer. In order to identify an endogenous tumor-associated Treg response, we analyzed the immune response in TRAMP mice, which develop prostatic adenocarcinoma due to the transgenic expression of the model oncogene SV40 T antigen in the prostate (4, 5). Unlike the prostates of tumor-free mice, which contain very few Treg cells (which are identified as CD4$^+$Foxp3$^+$), a substantial population of Tregs can be detected in the prostate tumors of TRAMP mice (fig. S1). We employed an experimental system involving T cell antigen receptor alpha chain (TCRα) repertoire analysis of T cell populations from TRAMP mice expressing the Foxp3^{gfp} reporter (6) and a fixed (transgenic) TCRβ chain. The fixed TCRβ used in this study was a TCRβ chain that was found to be

#Current Address: Department of Immunology, Harvard Medical School, Boston, MA 02115
*Current Address: Department of Immunology, The University of Texas MD Anderson Cancer Center, Houston, TX 77030

Supplementary Material www.sciencemag.org

recurrently expressed by $CD4^+Foxp3^+$ Tregs isolated from the prostates of TRAMP mice (fig. S2), and will be referred to hereafter as "TCRβtg". TCR complementarity determining region 3 (CDR3) length distribution analysis of cDNA from purified $CD4^+Foxp3^+$ and $CD4^+Foxp3^{neg}$ T cells from the prostate tumors of $TRAMP^{+/-}$ $Foxp3^{gfp}$ TCRβtg males revealed a substantial overrepresentation of $CD4^+Foxp3^+$ T cells expressing a Vα2 (TRAV14) TCRα chain with a CDR3 of nine amino acids in length (as defined by IMGT, http://www.imgt.org) (Fig. 1A, denoted in red). Deep sequencing of these samples revealed that the identical TCRα chain, of CDR3 sequence LYYNQGKLI, was recurrently expressed by $Foxp3^+$ Tregs (Fig. 1B), indicating that Tregs of a single specificity are recurrently enriched within TRAMP prostate tumors. Strikingly, in many prostate samples, the Vα2-LYYNQGKLI TCR chain was encoded by a single nucleotide sequence (fig. S3), suggesting that in many cases, tumor-infiltrating Tregs of this specificity may originate from a single clone.

A survey of different anatomical sites of $TRAMP^{+/-}$ $Foxp3^{gfp}$ TCRβtg mice using CDR3 length distribution analysis revealed that the overrepresentation of Tregs expressing a $Vα2^+$ TCRα chain of nine amino acids in length was observed in the prostate tumor and prostate-draining periaortic lymph nodes, but was not detected over background in non-draining brachial lymph nodes (Fig. 1C). Thus, Tregs of this specificity are not expanded systemically in tumor-bearing mice, but are instead selectively enriched in the prostate tumor environment.

In order to gain insight into the antigen specificities of polyclonal tumor-infiltrating $CD4^+$ T cells, we determined the extent of overlap of the $Vα2^+$ TCR repertoire for T cell subsets isolated from the prostate tumors of $TRAMP^{+/-}$ $Foxp3^{gfp}$ TCRβtg mice. Repertoire overlap was assessed using the Morisita-Horn (MH) similarity index (7–11), for which a value of 1 indicates identity, and a value of 0 denotes complete dissimilarity (Fig. 1D). The analysis revealed that the TCR repertoire of $CD4^+Foxp3^+$ and $CD4^+Foxp3^{neg}$ populations isolated from a particular prostate tumor were largely distinct and non-overlapping (MH = 0.07 ± 0.10 SD, Fig. 1D, samples intersecting at red lines), implying that the antigens recognized by tumor-infiltrating Tregs are different from those recognized by conventional $CD4^+$ T cells. Second, the TCR repertoire of $CD4^+Foxp3^+$ cells isolated from the prostates of different mice exhibited a high degree of similarity from mouse to mouse (MH = 0.38 ± 0.39 SD, Fig. 1D, upper left quadrant). While a substantial proportion of this similarity was due to the recurrent enrichment of the Vα2-LYYNQGKLI TCR, additional TCRα chains were identified that were recurrently expressed by prostatic $Foxp3^+$ Tregs (fig. S4). This finding suggests that TRAMP prostate tumors do not recruit polyclonal Tregs of arbitrary specificity, but instead are associated with the reproducible enrichment of Tregs of distinct specificities.

To facilitate the study of T cells expressing the canonical Vα2-LYYNQGKLI TCRα chain paired with the fixed TCRβ chain (hereafter referred to as "MJ23" T cells), we generated transgenic (tg) mice expressing the MJ23 TCRαβ heterodimer. In female MJ23tg *Rag1*$^{-/-}$ mice, $CD4^+$ T cells in the periphery were phenotypically naïve (Fig. 2A and fig. S5). Moreover, $Foxp3^+$ MJ23tg cells were not detected above background in the thymus and periphery of these mice (Fig. 2, A and B, and fig. S5). In contrast, analysis of tumor-free male MJ23tg *Rag1*$^{-/-}$ mice revealed spontaneous accumulation of activated $CD44^{hi}$ $CD4^+$ MJ23tg T cells in the prostate and prostate-draining periaortic lymph nodes (Fig. 2, A and B, and fig. S5), indicative of MJ23 reactivity to an autoantigen at these sites. In the prostate, T cell accumulation was observed in both the stroma and the epithelium, and was associated with disruption of the basement membrane of prostatic glands (Fig. 2C). The presence of activated $CD4^+$ T cells was accompanied by the concomitant appearance of a percentage of $CD4^+Foxp3^+$ T cells (Fig. 2, A and B, and fig. S5). $Foxp3^+$ cells exhibited *in vitro*

suppressive activity (fig. S6) and phenotypic characteristics of Tregs (fig. S7), including expression of neuropilin-1 (supplementary text and figs. S7 and S8). Taken together, our data demonstrate that MJ23 Tregs, identified based on their enrichment in mouse prostate tumors, are not reactive to a unique tumor-specific antigen, but instead recognize a self antigen associated with the organ of cancer origin.

In other experiments, $CD11c^+$ dendritic cells isolated from TRAMP prostate tumors induced robust proliferation of MJ23tg T cells *ex vivo* (Fig. 2D), but did not stimulate OT-II transgenic T cells expressing an irrelevant class II-restricted TCR (12). These data provide direct evidence that prostate tumors contain the antigen recognized by MJ23 T cells.

In order to study the development of MJ23tg T cells at physiological clonal frequencies, we generated chimeric animals in which bone marrow cells from MJ23tg *Rag1*$^{-/-}$ donors were engrafted into host mice at low frequencies (<1%), and the development and distribution of MJ23tg T cells was assessed (Fig. 3 and fig. S9). Analysis of B6 male and tumor-bearing TRAMP male hosts revealed that $Foxp3^+$ MJ23tg Tregs developed in the thymus (Fig. 3, A and B). The efficiency of development varied from mouse to mouse, and was inversely correlated with the frequency of MJ23tg precursors (Fig. 3B), a finding that is consistent with previously published studies (13, 14). In other experiments, OT-II *Rag1*$^{-/-}$ precursors did not develop efficiently into $Foxp3^+$ cells in the thymus, demonstrating the specificity of MJ23tg Treg development (fig. S10). In the periphery of male chimeras, $Foxp3^+$ MJ23tg cells were distributed throughout the secondary lymphoid organs, but were preferentially enriched in the prostate-draining periaortic lymph nodes (Fig. 3C), a finding consistent with evidence of reactivity to a prostate-associated antigen (Fig. 2). Very few donor-derived MJ23tg Tregs were observed in the prostate (Fig. 3, A and C), likely reflecting competition with endogenous MJ23 Tregs (supplementary text and fig. S11). Upon intravenous transfer of naïve $CD4^+Foxp3^{neg}$ MJ23tg T cells into TRAMP males, the induction of Foxp3 expression by MJ23tg cells was negligible (fig. S12), suggesting that antigen exposure in the periphery does not favor the development of induced Tregs. Taken together, our results demonstrate that expression of the MJ23 TCR facilitates Treg development in the thymus of male hosts. Thus, T cells of this specificity encounter the antigen(s) driving Treg development during maturation in the thymus, prior to their exposure to the prostate or tumor environment.

On the basis of our data indicating that MJ23 T cells are reactive to a prostate-associated antigen, we anticipated that $Foxp3^+$ MJ23tg Tregs would not develop in B6 female hosts. However, unexpectedly, $Foxp3^+$ MJ23tg Tregs developed in the thymus of chimeric B6 females (Fig. 3, A and B, and fig. S9). In the periphery of female mice, $Foxp3^+$ MJ23tg T cells were broadly distributed in the spleen and all lymph nodes examined, but selective enrichment in the periaortic lymph nodes was not observed in female hosts (Fig. 3C). In order to elucidate the mechanisms underlying MJ23tg Treg development in both male and female mice, we examined the role of Aire in development. *Aire* encodes a transcriptional regulator that drives the ectopic expression of peripheral tissue-specific antigens by medullary thymic epithelial cells, and is critical for the maintenance of immune tolerance (15–17). Analysis of MJ23tg development in chimeric mice in which MJ23tg precursors were engrafted into *Aire*$^{+/+}$ or *Aire*$^{-/-}$ hosts revealed that $Foxp3^+$ MJ23tg Tregs failed to develop in the thymus and periphery of *Aire*$^{-/-}$ hosts, both male and female (Fig. 4, A and B). In addition, *Aire*$^{-/-}$ hosts exhibited a reduction in the percentage of thymic Tregs relative to *Aire*$^{+/+}$ hosts, consistent with previous reports (15, 18), but were not characterized by a complete deficiency of polyclonal Tregs (Fig. 4, A and C). Despite the lack of MJ23tg Treg development, mature $CD4^+Foxp3^{neg}$ MJ23tg T cells developed in *Aire*$^{-/-}$ hosts (Fig. 4A and fig. S13), indicating that T cells of this specificity are not dependent on Aire for their positive selection into the $CD4^+$ lineage. This result also

suggests that the thymic development of Tregs reactive to an Aire-dependent antigen may require both the recognition of self peptide/MHC ligands for positive selection, and the recognition of an additional Aire-dependent antigen for commitment to the Treg lineage. Importantly, similar experiments utilizing a second naturally occurring tumor-infiltrating Treg TCR, termed "RT83", demonstrated that Aire is required for the thymic development of RT83tg Tregs (Fig. 4D and fig. S14). Thus, our data demonstrate that Aire is critical for the thymic development of multiple naturally occurring Treg specificities. These findings are consistent with a model in which the Aire-mediated expression of peripheral tissue-restricted antigens by thymic epithelial cells drives the development of a subset of tissue-specific or organ-specific Tregs (19).

While there is substantial evidence demonstrating that Aire plays a critical role in the deletion of autoreactive thymocytes reactive to peripheral tissue antigens (15, 20–22), a definitive role for Aire in the thymic selection of naturally occurring Tregs has not been previously established. Here, we provide direct evidence that Aire is critical for the thymic development of Tregs of naturally arising specificities. Thus, the integration of available evidence suggests a dual role for Aire in the maintenance of immune tolerance, in which Aire drives both the deletion of autoreactive T cells and the development of a subset of $Foxp3^+$ Tregs.

In sum, our data support a model in which a tumor does not drive the *de novo* conversion of tumor-specific $CD4^+$ effector T cells into induced $Foxp3^+$ Tregs, but instead recruits pre-existing thymic-derived Tregs reactive to Aire-dependent self antigens associated with the organ of cancer origin. Thus, a developing neoplasm co-opts endogenous mechanisms that have evolved to preserve the integrity of the host by maintaining organ-specific immune tolerance.

Supplementary Material

Refer to Web version on PubMed Central for supplementary material.

Acknowledgments

We thank A. Bendelac, T. Gajewski, R. Gottschalk, and S. Quezada for critical reading of the manuscript, A. Rudensky for $Foxp3^{gfp}$ reporter mice (6), C. Benoist for cassette vectors for TCRα and TCRβ transgenic mice (23), L. Degenstein for transgenic mouse production, and A. Thomas and N.-L. Yin for deep TCR sequence analysis. The data presented in this manuscript are tabulated in the main paper and in the supplementary materials. This work was partially funded by the following sources (to P.A.S.): R01 (#1R01CA160371-01), a Cancer Research Institute Investigator Award, a Cancer Research Foundation Young Investigator Award, an American Cancer Society Institutional Research Grant (#IRG-58-004), and the University of Chicago Comprehensive Cancer Center (including Support Grant #P30 CA14599). N.D.S. was supported by MSKCC Comprehensive Cancer Center (Support Grant #P30 CA008748). J.P.A. was supported by funding from the Howard Hughes Medical Institute.

References and Notes

1. Josefowicz SZ, Lu LF, Rudensky AY. Regulatory T cells: mechanisms of differentiation and function. Annu Rev Immunol. 2012; 30:531. [PubMed: 22224781]
2. Vesely MD, Kershaw MH, Schreiber RD, Smyth MJ. Natural innate and adaptive immunity to cancer. Annu Rev Immunol. 2011; 29:235. [PubMed: 21219185]
3. Deleeuw RJ, Kost SE, Kakal JA, Nelson BH. The Prognostic Value of FoxP3+ Tumor-Infiltrating Lymphocytes in Cancer: A Critical Review of the Literature. Clin Cancer Res. Jun 1.2012 18:3022. [PubMed: 22510350]
4. Greenberg NM, et al. Prostate cancer in a transgenic mouse. Proc Natl Acad Sci U S A. Apr 11.1995 92:3439. [PubMed: 7724580]

5. Gingrich JR, Barrios RJ, Foster BA, Greenberg NM. Pathologic progression of autochthonous prostate cancer in the TRAMP model. Prostate Cancer Prostatic Dis. Mar.1999 2:70. [PubMed: 12496841]
6. Fontenot JD, et al. Regulatory T cell lineage specification by the forkhead transcription factor foxp3. Immunity. Mar.2005 22:329. [PubMed: 15780990]
7. Wong J, Mathis D, Benoist C. TCR-based lineage tracing: no evidence for conversion of conventional into regulatory T cells in response to a natural self-antigen in pancreatic islets. J Exp Med. Sep 3.2007 204:2039. [PubMed: 17724131]
8. Wong J, et al. Adaptation of TCR repertoires to self-peptides in regulatory and nonregulatory CD4+ T cells. J Immunol. Jun 1.2007 178:7032. [PubMed: 17513752]
9. Hsieh CS, Zheng Y, Liang Y, Fontenot JD, Rudensky AY. An intersection between the self-reactive regulatory and nonregulatory T cell receptor repertoires. Nat Immunol. Apr.2006 7:401. [PubMed: 16532000]
10. Lathrop SK, Santacruz NA, Pham D, Luo J, Hsieh CS. Antigen-specific peripheral shaping of the natural regulatory T cell population. J Exp Med. Dec 22.2008 205:3105. [PubMed: 19064700]
11. Magurran. Ecological Diversity and Its Measurement. Princeton University Press; Princeton, NJ: 1988.
12. Barnden MJ, Allison J, Heath WR, Carbone FR. Defective TCR expression in transgenic mice constructed using cDNA-based alpha- and beta-chain genes under the control of heterologous regulatory elements. Immunol Cell Biol. Feb.1998 76:34. [PubMed: 9553774]
13. Bautista JL, et al. Intraclonal competition limits the fate determination of regulatory T cells in the thymus. Nat Immunol. Jun.2009 10:610. [PubMed: 19430476]
14. Leung MW, Shen S, Lafaille JJ. TCR-dependent differentiation of thymic Foxp3+ cells is limited to small clonal sizes. J Exp Med. Sep 28.2009 206:2121. [PubMed: 19737865]
15. Anderson MS, et al. The cellular mechanism of Aire control of T cell tolerance. Immunity. Aug. 2005 23:227. [PubMed: 16111640]
16. Anderson MS, et al. Projection of an immunological self shadow within the thymus by the aire protein. Science. Nov 15.2002 298:1395. [PubMed: 12376594]
17. Mathis D, Benoist C. Aire. Annu Rev Immunol. 2009; 27:287. [PubMed: 19302042]
18. Lei Y, et al. Aire-dependent production of XCL1 mediates medullary accumulation of thymic dendritic cells and contributes to regulatory T cell development. J Exp Med. Feb 14.2011 208:383. [PubMed: 21300913]
19. Aschenbrenner K, et al. Selection of Foxp3+ regulatory T cells specific for self antigen expressed and presented by Aire+ medullary thymic epithelial cells. Nat Immunol. Apr.2007 8:351. [PubMed: 17322887]
20. Liston A, Lesage S, Wilson J, Peltonen L, Goodnow CC. Aire regulates negative selection of organ-specific T cells. Nat Immunol. Apr.2003 4:350. [PubMed: 12612579]
21. Taniguchi RT, et al. Detection of an autoreactive T-cell population within the polyclonal repertoire that undergoes distinct autoimmune regulator (Aire)-mediated selection. Proc Natl Acad Sci U S A. May 15.2012 109:7847. [PubMed: 22552229]
22. DeVoss J, et al. Spontaneous autoimmunity prevented by thymic expression of a single self-antigen. J Exp Med. Nov 27.2006 203:2727. [PubMed: 17116738]
23. Kouskoff V, Signorelli K, Benoist C, Mathis D. Cassette vectors directing expression of T cell receptor genes in transgenic mice. J Immunol Methods. Mar 27.1995 180:273. [PubMed: 7714342]
24. Materials and methods are available as supplementary materials in Science Online.

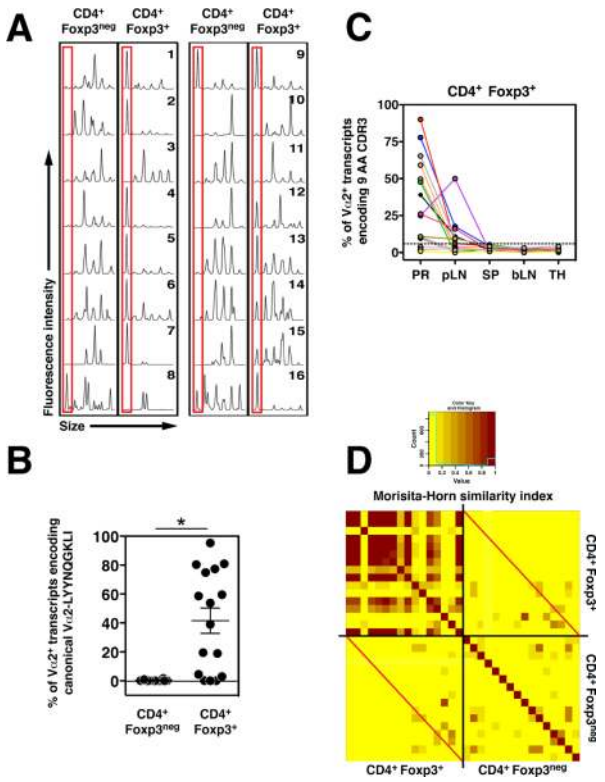

Fig. 1. CD4$^+$Foxp3$^+$ Tregs expressing a canonical TCR are recurrently enriched in TRAMP prostate tumors

Analysis of Vα2 (TRAV14)$^+$ TCRα chains in tumor-bearing TRAMP$^{+/-}$ Foxp3^{gfp} TCRβtg mice. CD4$^+$Foxp3^{neg} and CD4$^+$Foxp3$^+$ T cells were FACS-purified from different anatomical sites of ~27-week-old male mice, and cDNA was subjected to molecular analysis. **(A)** CDR3 length distribution analysis of Vα2$^+$ TCRα chains of T cell subsets isolated from prostate tumors. The mouse number is indicated. The red boxes denote TCRα transcripts encoding a CDR3 of 9 amino acids (AA) in length. **(B)** Vα2$^+$ TCRα transcripts from the indicated populations were PCR amplified and subjected to deep sequencing (see Methods (24)). The percentage of all Vα2$^+$ TCRα transcripts encoding the canonical Vα2-LYYNQGKLI chain is plotted for each sample. The mean ± SEM is indicated. The asterisk indicates $p < 0.05$ (t-test). **(C)** Plots of the percentage of Vα2$^+$ transcripts encoding a CDR3 of 9 AAs (based on peak area) for CD4$^+$Foxp3$^+$ T cells isolated from different anatomical sites of the mice depicted in panel (A). PR, prostate; pLN, periaortic lymph nodes; SP, spleen; bLN, brachial lymph nodes; TH, thymus. Samples from each mouse are color-coded. The plot does not depict data from mice 1 and 2, and includes data from two additional mice (numbers 17 and 18). Samples with values above the indicated threshold (dashed line) are considered "overrepresented". This threshold is defined as the mean percent peak area plus three standard deviations for Vα2$^+$ TCRα transcripts encoding a 9 AA CDR3 from the spleen of female TCRβtg mice. **(D)** Heat map of the Morisita-Horn (MH) similarity index for prostatic T cell subsets from mice 1–16. Samples are oriented in ascending numerical order, from top to bottom and left to right (not shown). A motif table of predicted amino acid sequences is presented in Table S1. CD4$^+$Foxp3^{neg} and CD4$^+$Foxp3$^+$ subsets from the same prostate tumor intersect at the red diagonal lines. Data are pooled from $N = 3$ independent FACS-sorting experiments.

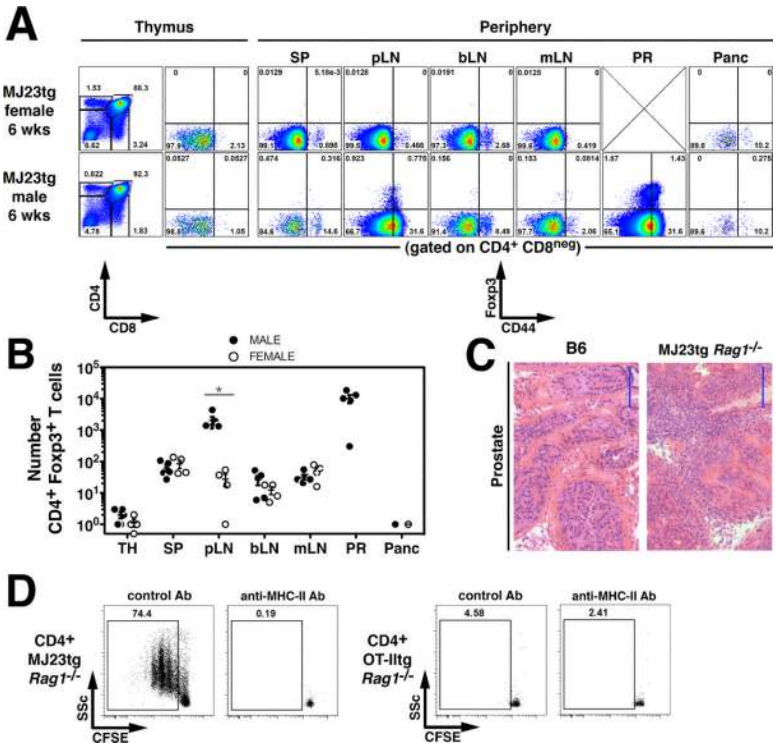

Fig. 2. MJ23 T cells recognize a prostate-associated self antigen

(A–C) Spontaneous T cell autoreactivity in the prostates of tumor-free male MJ23tg *Rag1*$^{-/-}$ mice. **(A)** Representative flow cytometric analyses of T cells isolated from the indicated organs of 6-week-old male or female mice. SP, spleen; pLN, periaortic lymph nodes; bLN, brachial lymph nodes; mLN, mesenteric lymph nodes; PR, prostate; Panc, pancreas. **(B)** Summary plot of the absolute number of CD4^{+}Foxp3^{+} T cells from the indicated organs of 6-week-old male or female mice. **(C)** Hematoxylin and eosin staining of dorsolateral prostatic lobes from 18-week-old MJ23tg *Rag1*$^{-/-}$ and B6 mice. Scale bar = 100 μm. **(D)** CFSE-labeled CD4^{+}Foxp3^{neg} MJ23tg T cells or OT-IItg cells were cultured with FACS-purified CD45^{+}CD11c^{+}F4/80^{neg} cells isolated from TRAMP prostate tumors in the presence of recombinant mouse IL-2. In addition, MHC-II antibody or isotype control antibody was added to the culture. Dilution of CFSE was assessed by flow cytometry on day 4. The mean ± SEM is indicated. Asterisks indicate $p < 0.05$, ns = not significant. For (A–B), data are pooled from $N = 2$ independent experiments. For (B), t-tests were used to compare data from male and female mice at each site. Data in (D) are representative of $N = 7$ independent experiments.

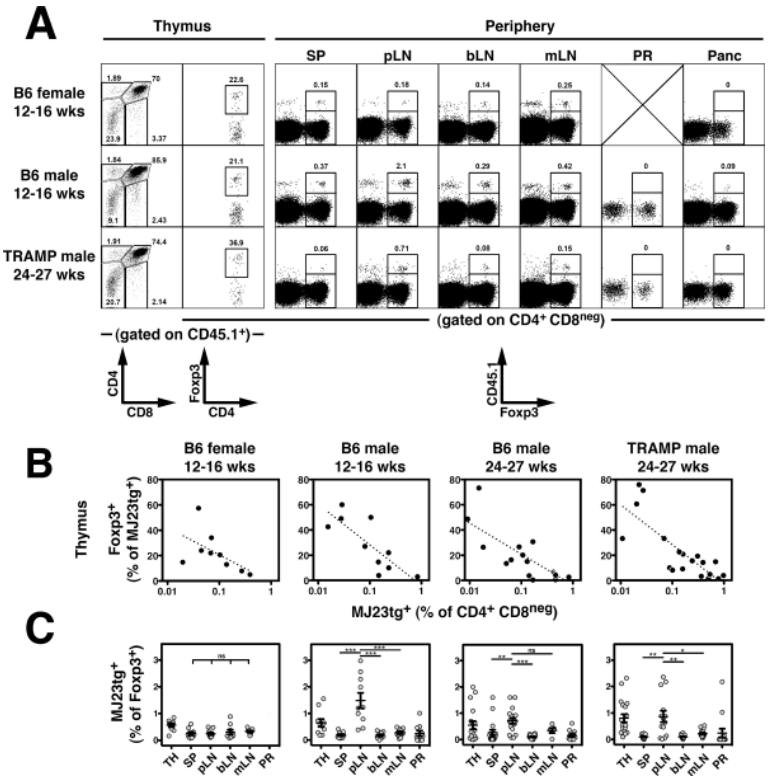

Fig. 3. Thymic development of MJ23 Tregs

The MJ23 TCR facilitates thymic Treg development at low clonal frequencies. T cell-depleted bone marrow cells from MJ23tg *Rag1*$^{-/-}$ CD45.1^{+} female donor mice were engrafted, along with polyclonal "filler" cells from B6 females (CD45$^{.2/.2}$), into sublethally irradiated CD45$^{.2/.2}$ recipient mice. This approach resulted in seeding of MJ23tg precursors at a low frequency (<1%). 6 weeks post-engraftment, the fate of MJ23tg cells was analyzed. **(A)** Representative flow cytometric analyses of CD45.1^{+} MJ23tg T cells from different anatomical sites of male or female mice of the indicated ages and strain. Abbreviations are the same as in Fig. 2. For the thymus, the left column (CD4 vs. CD8) depicts undepleted samples, the right column (Foxp3 vs. CD4) depicts CD8-depleted samples. For the periphery, the percentage of all CD4^{+}Foxp3^{+} T cells that are CD45.1^{+} (MJ23tg^{+}) is indicated. **(B)** Summary plots of the "efficiency" of MJ23tg Treg development in the thymus, in which the percentage of CD4^{+}CD8^{neg} CD45.1^{+} MJ23tg cells that express Foxp3 is plotted vs. the frequency of CD45.1^{+} MJ23tg thymocytes (as a percentage of all CD4^{+}CD8^{neg} cells) for cells isolated from host mice of the indicated strain, gender, and age. Dashed lines indicate best-fit semi-log curves. **(C)** Summary plots of the percentage of CD45.1^{+} MJ23tg T cells amongst all CD4^{+}Foxp3^{+} cells isolated from various organs of the indicated hosts. The mean ± SEM is shown. Asterisks indicate $p < 0.05$. ANOVA was used to compare the secondary lymphoid sites (spleen and lymph nodes) within chimeric hosts of a given type. Data are pooled from at least $N = 3$ independent experiments.

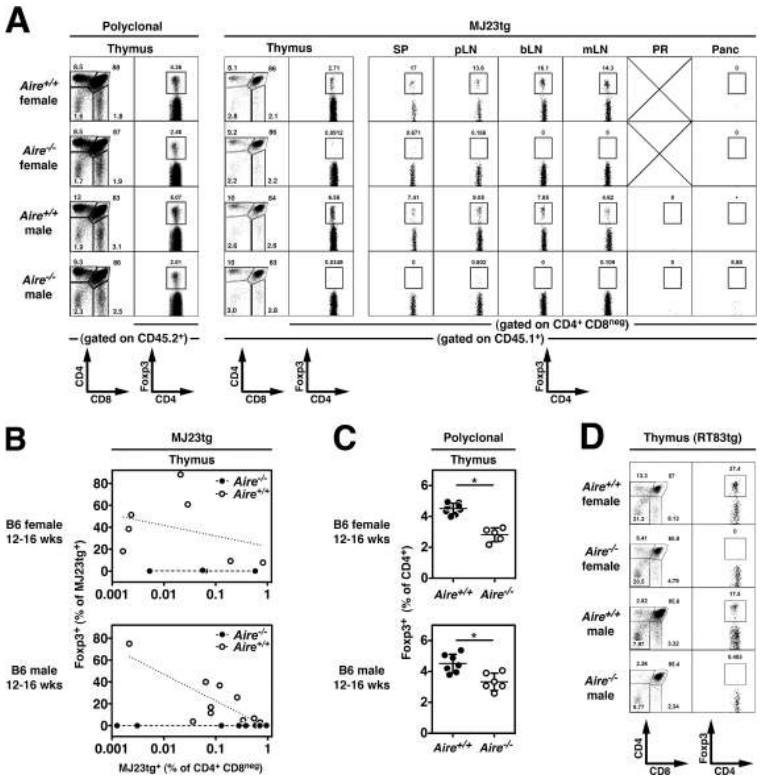

Fig. 4. Aire-dependent thymic development of antigen-specific Tregs

(A–C). The thymic development of MJ23tg Tregs is Aire-dependent. T cell-depleted bone marrow cells from MJ23tg *Rag1*$^{-/-}$ CD45.1^{+} female donor mice were engrafted, along with "filler" cells from *Aire*$^{-/-}$ females (CD45$^{.2/.2}$), into sublethally irradiated *Aire*$^{-/-}$ or *Aire*$^{+/+}$ recipient mice (CD45$^{.2/.2}$), both male and female. 6 weeks post-engraftment, the fate of MJ23tg cells was analyzed. **(A)** Representative flow cytometric analyses of CD45.2^{+} polyclonal T cells (left) and CD45.1^{+} MJ23tg T cells from different anatomical sites of 12–16-week-old male or female mice of the indicated *Aire* genotype. Abbreviations are the same as in Fig. 2. The percentage of CD4^{+} cells that are Foxp3^{+} is shown. For the thymus, the left column (CD4 vs. CD8) depicts undepleted samples, the right column (Foxp3 vs. CD4) depicts CD8-depleted samples. **(B)** Summary plots of the "efficiency" of MJ23tg Treg development, in which the percentage of CD45.1^{+} MJ23tg cells that express Foxp3 is plotted vs. the frequency of CD45.1^{+} MJ23tg thymocytes (as a percentage of all CD4^{+}CD8^{neg} cells) for cells isolated from host mice of the indicated sex and genotype. Dashed lines indicate best-fit semi-log curves. **(C)** Summary plots of the percentage of CD45.2^{+} polyclonal CD4^{+}CD8^{neg} thymocytes that express Foxp3 in chimeric mice of the indicated sex and genotype. The mean ± SEM is shown. Asterisks indicate $p < 0.05$ for the comparison of *Aire*$^{-/-}$ vs. *Aire*$^{+/+}$ mice (t-test). Data in (A–C) are pooled from $N = 3$ independent experiments. **(D)** Aire-dependent thymic development of "RT83tg" Tregs. RT83tg bone marrow chimeras were generated in *Aire*$^{-/-}$ or *Aire*$^{+/+}$ hosts, as described above for MJ23tg T cells. Representative flow cytometric analyses of CD45.1^{+} RT83tg T cells from the thymus of 12–16-week-old male or female mice of the indicated *Aire* genotype. The percentage of CD4^{+} cells that are Foxp3^{+} is shown. For the thymus, the left column (CD4 vs. CD8) depicts undepleted samples, the right column (Foxp3 vs. CD4) depicts CD8-depleted samples. Data in (D) are pooled from $N = 2$ independent experiments.